Phases of unitary matrix models and lattice QCD_2

Jorge G. Russo*

Institució Catalana de Recerca i Estudis Avançats (ICREA), Pg. Lluis Companys, 23, 08010 Barcelona, Spain and Departament de Física Cuántica i Astrofísica and Institut de Ciències del Cosmos, Universitat de Barcelona, Martí Franquès, 1, 08028 Barcelona, Spain

(Received 13 October 2020; accepted 5 November 2020; published 23 November 2020)

We investigate the different large N phases of a generalized Gross-Witten-Wadia (GWW) $U(N)$ matrix model. The deformation mimics the one-loop determinant of fermion matter with a particular coupling to gauge fields. In one version of the model, the GWW phase transition is smoothed out and it becomes a crossover. In another version, the phase transition occurs along a critical line in the two-dimensional parameter space spanned by the 't Hooft coupling λ and the Veneziano parameter τ. We compute the expectation value of Wilson loops in both phases, showing that the transition is third order. A calculation of the β function shows the existence of an IR stable fixed point.

DOI: 10.1103/PhysRevD.102.105019

I. INTRODUCTION

The study of random matrix ensembles caters to a broad variety of most diverse applications in different areas of physics and mathematics [1–3]. In a recent paper [4], a new unitary one-matrix model was constructed and investigated. The model has the potential

$$V = -\frac{1}{g^2}\mathrm{Tr}(U+U^\dagger) + 2\nu \mathrm{Tr}\,\ln(2+U+U^\dagger). \quad (1)$$

It represents a natural deformation of the Gross-Witten-Wadia (GWW) model [5,6] and it interpolates between classical unitary matrix models. The theory exhibits various large N phase transitions in the parameter space of the two couplings, with an intricate structure that has been only partially investigated in [4], and it is the unitary counterpart of the Hermitian, deformed-Cauchy random matrix ensemble [7]. This contains one Hermitian matrix M subject to the potential

$$V_H = A\mathrm{Tr}\,\ln(1+M^2) + B\mathrm{Tr}\frac{1}{1+M^2}. \quad (2)$$

The term with coefficient A corresponds to the logarithmic term in (1) (taking into account a shift due to the Jacobian of the stereographic map), while the term with coefficient B gives rise to the GWW term. The model generalizes the Hermitian model appeared in [8], derived from the $\nu = 0$ case (see [9,10] for earlier studies on related models). The logarithmic term appears in the mathematical literature in the study of Cauchy random matrix ensembles [11]. Above a certain critical value of the coupling B, the potential develops a double well, leading to a phase transition. In this paper, we will describe in detail the analogous phase transition in the unitary model (1), which exhibits some striking features. One phase was already described in [4]. Here we will find the explicit solution for both phases and compute some relevant observables.

The logarithmic term with coefficient ν corresponds to an insertion

$$[\det(2+U+U^\dagger)]^\nu = [\det(1+U)(1+U^\dagger)]^\nu. \quad (3)$$

A related deformation is obtained by the insertion of the operator

$$[\det(2-U-U^\dagger)]^\nu = [\det(1-U)(1-U^\dagger)]^\nu. \quad (4)$$

This is equivalent to the deformation (3) if at the same time the sign of the coupling is flipped, $g^2 \to -g^2$ and $U \to -U$. However, when viewed as deformations of the GWW matrix model, the physical interpretation of both models is different. In particular, the insertion (3) leads to smoothing out the GWW phase transition occurring in the physical range of the coupling $g^2 > 0$, whereas the insertion (4) leads to extending the GWW third-order phase transition to a critical line in the two-dimensional parameter space of couplings. In addition, $U \to -U$ flips the sign of the Wilson loop.

*jorge.russo@icrea.cat

An important question concerns the possible physical interpretation of the deformation in the context of two-dimensional lattice gauge theory. The determinantal form of the insertion, with $\nu > 0$, suggests the obvious interpretation as a one-loop fermion determinant. In conventional lattice QCD_2, one has the Wilson fermions with action [12]

$$S = \sum_{n,m} \bar{\psi}_n K(n,m) \psi_m, \tag{5}$$

$$K(n,m) = \delta_{nm} - \frac{1}{2(2r+m_0)} \sum_{\mu} [(r-\gamma_\mu) U_\mu(n) \delta_{n+\mu,m} + (r+\gamma_\mu) U_\mu^\dagger(m) \delta_{n-\mu,m}], \tag{6}$$

where r contributes to the energy of spurious fermion modes and m_0 represents the bare quark mass. The fermion determinant is complicated and finding the meson spectrum requires elaborated calculations based on Monte Carlo [12]. On the other hand, the insertion (3) is equivalent to

$$\int D\psi D\bar{\psi} e^{\sum_{i=1}^{N_f} \bar{\psi}_i (2+U+U^\dagger)\psi_i}, \qquad N_f \equiv \nu/2. \tag{7}$$

The determinant (3) is clearly much simpler than the one in the more realistic model (6), as it only includes variables in a single plaquette: like in the GWW matrix model, the full partition function would be obtained as Z^{V/a^2}, where V is the volume of space and a is the lattice spacing. However, similar (but still more complicated) determinants appear in Eguchi-Kawai reductions [13] involving Wilson fermion determinants [14,15]. In particular, for N_f adjoint fermions, the adjoint Eguchi-Kawai model has a single-site Wilson fermion operator D_W given by [16]

$$D_W = 1 - \kappa \sum_{i=1}^{4} [(1-\gamma_\mu) U_\mu^{\mathrm{adj}} + (1+\gamma_\mu) U_\mu^{\dagger \mathrm{adj}}]. \tag{8}$$

Computing physical quantities in this model, such as Wilson loop expectation values, still requires heavy numerical calculations [16]. On the other hand, the present model can be fully solved by analytic methods, including $1/N$ effects, and it might provide a simple phenomenological setup to reproduce some features of QCD_2.

A different strategy is to write the bilinear fermion term in (7) as a gauge-invariant term in the form

$$\overline{\psi}_i (1 + \prod_P U + \mathrm{H.c.}) \psi_i, \tag{9}$$

where the product $\prod_P$ represents the square plaquette containing the original link variables prior to the Weyl gauge fixing $U_{\vec{n},\vec{1}_0} = 1$, $\vec{1}_0$ being the lattice vector in the time direction. In the continuum, the plaquette is associated with the operator $\mathrm{Tr} e^{ia^2 \hat{F}_{01}}$ (see e.g., [17]). This naturally leads to an expansion in the bilinear fermion term having higher-dimensional couplings such as $\bar{\psi} \hat{F}_{\mu\nu} \hat{F}^{\mu\nu} \psi$. Thus, according to this view, the insertion (3) would seem to compute the effect of such deformations together with a mass term, in sectors where the fermion kinetic energy may be negligible.

Another interesting interpretation of the deformation in (1) arises in the context of $SU(N)$ Yang-Mills theory on S^3 [18,19]. Expanding the new term in powers of U, $U^\dagger$, one has

$$\mathrm{Tr} \ln (2 + U + U^\dagger) = -\sum_{k=1}^{\infty} \frac{(-1)^k}{k} (\mathrm{Tr} U^k + \mathrm{Tr} U^{\dagger k}). \tag{10}$$

This operator plays a special role in the black hole/string phase transition as it represents a gap opening perturbation added to the action [20]. It would be extremely interesting to explore the consequences of our results in that context.

This paper is organized as follows. In Sec. II, we introduce the matrix models A and B corresponding to insertions (3) and (4) and study them in a large N double-scaling limit. The eigenvalue densities for models A and B in the two different phases are determined in Secs. I and II B. The resulting phase diagram is shown in Fig. 4. In Sec. III, we compute the free energy, the vacuum expectation value of Wilson loops and winding Wilson loops in the weak- and strong-coupling phases of model B and determine the order of the phase transition. Finally, in Sec. IV, we compute the β function. In model B, it exhibits the presence of IR stable fixed points.

II. THE UNITARY MATRIX MODEL

We shall consider two deformations of lattice $U(N)$ gauge theory in two dimensions. The first model A has partition function

$$Z^A = \int dU \det \left(\frac{1}{4} (2 + U + U^\dagger) \right)^\nu e^{\frac{1}{g^2} \mathrm{Tr}(U+U^\dagger)}. \tag{11}$$

Integrating over the volume of the group, this becomes

$$Z^A = \frac{1}{N!} \int_{(0,2\pi]^N} \prod_{1 \le j < k \le N} |e^{i\varphi_j} - e^{i\varphi_k}|^2 \prod_{j=1}^{N} \cos^{2\nu} \left(\frac{\varphi_j}{2} \right) \times \exp \left(\frac{2}{g^2} \cos(\varphi_j) \right) \frac{d\varphi_j}{2\pi}. \tag{12}$$

The second model B has partition function

$$Z^B = \int dU \det \left(\frac{1}{4} (2 - U - U^\dagger) \right)^\nu e^{\frac{1}{g^2} \mathrm{Tr}(U+U^\dagger)}. \tag{13}$$

In this case, one gets

$$Z^B = \frac{1}{N!}\int_{(0,2\pi]^N} \prod_{1\le j<k\le N} |e^{i\varphi_j} - e^{i\varphi_k}|^2 \prod_{j=1}^{N} \sin^{2\nu}\left(\frac{\varphi_j}{2}\right) \times \exp\left(\frac{2}{g^2}\cos(\varphi_j)\right)\frac{d\varphi_j}{2\pi}. \quad (14)$$

The two models are mathematically equivalent as they are related by changing $g^2 \to -g^2$ and shifting the φ_j integration variables by π. However, their physical interpretation as a deformation of the GWW model is different. Considering $g^2 > 0$, the deformation of the potential in terms of $\ln \sin^2\frac{\varphi}{2}$—instead of $\ln\cos^2\frac{\varphi}{2}$—implies a stronger deformation in the region of small eigenvalues. As a result, this will lead to a very different deviation from the GWW model: in model A, the large N GWW phase transition is smoothed out and it becomes a crossover [4]. In model B, the large N GWW phase transition subsists. In addition, there are some striking consequences for observables and for the β function of the running coupling.

We are interested in the large N "Veneziano" limit with fixed parameters

$$\lambda \equiv g^2 N, \qquad \tau \equiv \frac{\nu}{N}. \quad (15)$$

Thus, we have unitary one-matrix models with potentials

$$V^A = -\frac{2}{\lambda}\cos(\alpha) - \tau \ln\cos^2\frac{\alpha}{2}, \quad (16)$$

$$V^B = -\frac{2}{\lambda}\cos(\alpha) - \tau \ln\sin^2\frac{\alpha}{2}. \quad (17)$$

Here we assume that $\tau \ge 0$ (a discussion of the phase diagram in the region $\tau < 0$ is given in [4]). A partial analysis was carried out in [4], where it was found that these models have two phases. The phase transition occurs on a critical line $\lambda_{\rm cr}(\tau)$, which for model B lies on the region $\lambda > 0$. As only one phase was described explicitly in [4], here we will complete this analysis by explicitly deriving the solution in the two phases and by computing the free energy and some relevant physical observables.

A. Eigenvalue distribution for model A

At large N, the partition function is determined by a saddle-point calculation. The large N regime is studied as usual by introducing a unit-normalized density of eigenvalues $\rho(\alpha)$. The saddle-point equation then becomes the singular integral equation

$$\frac{2}{\lambda}\sin\alpha + \tau\tan\frac{\alpha}{2} = P\int_L d\beta\rho(\beta)\cot\left(\frac{\alpha-\beta}{2}\right), \quad (18)$$

where L represents the region where eigenvalues condense. The dynamics governing the eigenvalues can be understood by examining the behavior of the potential in the parameter space.

Consider, in first place, positive λ. In this case, both terms of the potential (16) give a force driving eigenvalues to the region near $\alpha = 0$. For small λ, the force is large and eigenvalues must get condensed in a small cut, with an eigenvalue distribution that must approach the GWW eigenvalue distribution, since the deformation is negligible compared with the first term. As λ is increased, the cut gets wider. However, as long as $\tau > 0$, eigenvalues cannot get to $\pm\pi$ because the potential grows to infinity at $\pm\pi$ owing to the deformation. This is a crucial effect, which removes the GWW phase transition transforming it into a crossover.

On the other hand, for negative λ, the force associated with the sine term in (18) becomes repulsive. As a result, there is a critical coupling beyond which the potential develops a double well. This occurs at $\lambda_1 = -4/\tau$. At this point, the eigenvalue distribution is still described by a one-cut solution, due to overfilling of eigenvalues (a fact that will be verified below). By further increasing λ, one meets another critical value $\lambda_{\rm cr}$, where the eigenvalue distribution is split into two cuts. Below we explicitly describe the two regimes.

1. The one-cut phase in model A

Let us first review the main features of the one-cut solution found in [4]. This phase is described by the solution

$$\rho(\alpha) = \left(\frac{2}{\pi\lambda}\cos\frac{\alpha}{2} + \frac{\tau}{2\pi}\frac{1}{\sqrt{1-m}\cos\frac{\alpha}{2}}\right)\sqrt{m - \sin^2\frac{\alpha}{2}}. \quad (19)$$

The cut extends in the interval $(-\alpha_0, \alpha_0)$, with $m = \sin^2\alpha_0/2$, $|\alpha_0| < \pi$, $0 < m < 1$. When $\tau = 0$, the solution (19) reduces to the familiar solution of the GWW model in the gapped phase. The parameter m determines the width of the eigenvalue distribution. It is easily found from the normalization condition

$$1 = \int_{-\alpha_0}^{\alpha_0} d\beta\rho(\beta) = \frac{2m}{\lambda} + \left(\frac{1}{\sqrt{1-m}} - 1\right)\tau, \quad (20)$$

which leads to a cubic equation for m. For all $\tau > 0$, there is a unique real root with $0 < m < 1$, which determines $m = m(\lambda, \tau)$. A simple way to see this is by solving the normalization condition for τ. This gives

$$\tau = \frac{\sqrt{1-m}(\lambda - 2m)}{\lambda(1-\sqrt{1-m})}. \quad (21)$$

For small $m > 0$, one has $\tau \sim 2/m \gg 1$. Then τ monotonically decreases until it vanishes. Thus, for any positive τ, there is a unique value of m satisfying (21).

As discussed above, the phase described by (19) subsists until a critical point beyond which ρ becomes negative in some interval $\subset (-\alpha_0, \alpha_0)$, due to the fact that the potential develops a double well. At the critical point, the density ρ vanishes at the origin $\alpha = 0$. This gives the condition

$$\frac{2}{\pi\lambda} + \frac{\tau}{2\pi}\frac{1}{\sqrt{1-m}} = 0 \to \tau\lambda_{\rm cr} = -4\sqrt{1-m}. \quad (22)$$

In particular, this shows that $0 > \lambda_{\rm cr} > \lambda_1$. Since m is a function of λ and τ, the critical coupling $\lambda_{\rm cr}$ is a function of τ. Indeed, combining with (21), we obtain

$$\lambda_{\rm cr} = -\frac{4}{\tau^2}(\tau + 1 - \sqrt{2\tau+1}), \quad (23)$$

or

$$\frac{2}{\lambda_{\rm cr}} = -\frac{1}{2}(\tau + 1 + \sqrt{2\tau+1}). \quad (24)$$

Thus, the eigenvalue density is described by the solution (19) in the regime $\lambda \in \{-\infty, \lambda_{\rm cr}\} \cup \{0, \infty\}$.

Note that, for $\tau \to 0$, one has $\lambda_{\rm cr} \to -2$. This is nothing but the GWW phase transition in a frame where the sign of λ has been flipped by shifting the eigenvalues by π. On the other hand, the GWW phase transition occurring at $\tau = 0$, $\lambda = 2$ is smoothed out by the deformation. For any $\tau > 0$, the free energy in the region $\lambda > 0$ is analytic, since the solution does not change in this region of the plane (τ, λ). Of course, the phase transition at $\lambda = 2$ remains on the axis $\tau = 0$.

2. The two-cut phase in model A

In the regime $0 > \lambda > \lambda_{\rm cr}$, the eigenvalue distribution is split into two cuts, implying a phase transition. The phase transition is the unitary matrix model counterpart of the phase transition found in [7], in the Hermitian matrix model version. The solutions of unitary and Hermitian matrix models are connected by a simple map described in [21] (see also the Appendix in [22]). Alternatively, one can solve (18) directly by standard methods for one-matrix models. For the two-cut solution, we obtain

$$\rho(\alpha) = \frac{\tau}{4\pi}\sqrt{\sin^2\alpha}\sqrt{a^2 - \tan^2\frac{\alpha}{2}}\sqrt{\tan^2\frac{\alpha}{2} - b^2}. \quad (25)$$

The parameters a, b representing the end points of the eigenvalue distribution may be obtained from two conditions arising from normalization and from the integral equation (18) itself. To compute integrals and check the equations, it is convenient to introduce the variable $t = e^{i\alpha}$. Then

$$\rho(\alpha)d\alpha = \hat{\rho}(t)dt, \quad (26)$$

with

$$\hat{\rho}(t) = \frac{\tau}{8\pi}\frac{(1-t)}{(1+t)t^2}\sqrt{4t - (1+b^2)(1+t)^2} \times \sqrt{a^2(1+t)^2 + (t-1)^2}. \quad (27)$$

We first demand normalization,

$$\int_L dt\hat{\rho}(t) = 1. \quad (28)$$

The integral goes over the two cuts in the circle described by t, $L = (\alpha_0, \alpha_1) \cup (-\alpha_1, -\alpha_0)$. The integral can be computed by residues, by considering two contours, surrounding each branch cut. Then the integral picks the residue of the poles at $t = 0$, $t = -1$, and $t = \infty$, that is,

$$\int_L dt\hat{\rho}(t) = i\pi(\mathrm{Res}_{t=0}\hat{\rho}(t) + \mathrm{Res}_{t=-1}\hat{\rho}(t) + \mathrm{Res}_{t=\infty}\hat{\rho}(t)). \quad (29)$$

We obtain the condition

$$1 = \tau\left(\frac{2 + a^2 + b^2}{2\sqrt{1+a^2}\sqrt{1+b^2}} - 1\right). \quad (30)$$

Let us now consider the integral equation (18). In terms of t, it is given by

$$\frac{2}{\lambda}\sin\alpha + \tau\tan\frac{\alpha}{2} = -i\int_L dt\hat{\rho}(t)\frac{t + e^{i\alpha}}{t - e^{i\alpha}}. \quad (31)$$

Choosing the same contours surrounding the cuts, the integration by residues now gives

$$-i\int_L dt\hat{\rho}(t)\frac{t + e^{i\alpha}}{t - e^{i\alpha}} = -\frac{\tau}{2}\sqrt{1+a^2}\sqrt{1+b^2}\sin\alpha + \tau\tan\frac{\alpha}{2}. \quad (32)$$

Therefore, we get the second condition on the parameters a, b,

$$\frac{2}{\lambda} = -\frac{\tau}{2}\sqrt{1+a^2}\sqrt{1+b^2}. \quad (33)$$

The solution to (30), (33) is

$$1 + a^2 = -\frac{4(1 + \tau + \sqrt{2\tau+1})}{\lambda\tau^2}, \quad (34)$$

$$1 + b^2 = -\frac{4(1 + \tau - \sqrt{2\tau+1})}{\lambda\tau^2}. \quad (35)$$

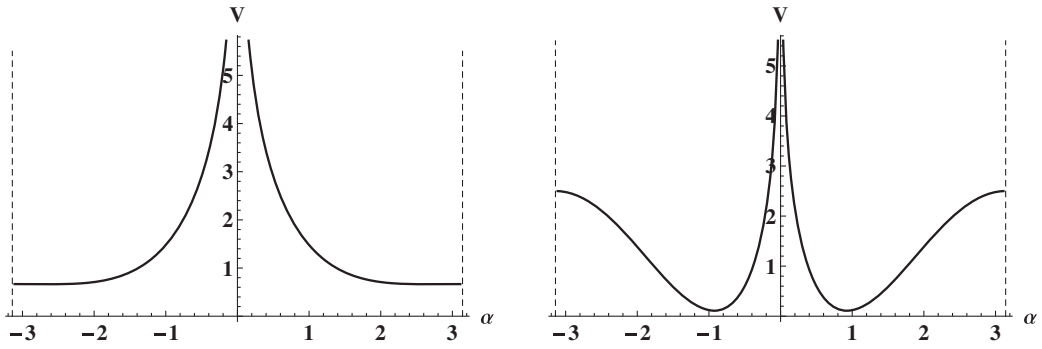

FIG. 1. The potential in model B. (a) In the supercritical phase, with $\lambda = 3$, $\tau = 1.25$. (b) In the subcritical phase, with $\lambda = 0.8$, $\tau = 1$.

These values of a, b coincide, as expected, with the values of a, b of the Hermitian model in [7], taking into account the shift $\tau \to \tau - 1$.[1]

The critical line occurs when $b = 0$. This gives

$$\lambda_{\rm cr}(\tau) = -\frac{4}{\tau^2}(\tau + 1 - \sqrt{2\tau + 1}). \tag{36}$$

This critical line exactly coincides with the critical line obtained from the one-cut phase. Moreover, we can check continuity on the critical line. Setting $\lambda = \lambda_{\rm cr}(\tau)$, on the critical line, the eigenvalue density (25) simplifies to

$$\rho_{\rm cr} = \frac{\tau}{2\pi}\frac{\sin^2\frac{\alpha}{2}}{\cos\frac{\alpha}{2}}\sqrt{a^2 - (1+a^2)\sin^2\frac{\alpha}{2}}. \tag{37}$$

This matches the critical density obtained from the solution in phase 1, noticing that

$$m_{\rm cr} = \frac{a^2}{1+a^2}, \qquad \lambda_{\rm cr}\tau = -4\sqrt{1 - m_{\rm cr}}. \tag{38}$$

B. Eigenvalue distribution for model B

We now consider the matrix model defined by the GWW partition function with the insertion $\det(\frac{1}{4}(2 - U - U^\dagger))^\nu$, leading to (14). At large N, the saddle-point equations are equivalent to the integral equation

$$\frac{2}{\lambda}\sin\alpha - \tau\cot\frac{\alpha}{2} = P\int_L d\beta\rho(\beta)\cot\left(\frac{\alpha-\beta}{2}\right). \tag{39}$$

Using the connection to model A by $\lambda \to -\lambda$, one finds that the model B (14) has two phases in the region $\lambda > 0$, separated by a critical line

$$\lambda_{\rm cr} = \frac{4}{\tau^2}(\tau + 1 - \sqrt{2\tau + 1}). \tag{40}$$

Note that $\lambda_{\rm cr} \to 2$ when $\tau \to 0$.

The origin of the two phases can be understood by looking at the potential, which has a double-well for sufficiently small λ, thus inducing the phase transition from a one-cut to a two-cut distribution (see Fig. 1). There is a sharp distinction with the potential in the GWW model. In model B, a "wall" appears at *small* eigenvalues, which becomes infinitely thin as $\tau \to 0$, where the physics of the GWW model is recovered. Below we describe the eigenvalue densities for the two phases.

1. One-cut phase in model B ($\lambda > \lambda_{\rm cr}$)

In the strong-coupling phase $\lambda > \lambda_{\rm cr}$, eigenvalues condense in one cut. The density is obtained from (19) by using the map $\lambda \to -\lambda$, $\alpha \to \alpha \pm \pi$. One obtains[2]

$$\rho_{1\,\rm cut}(\alpha) = \left(-\frac{2}{\pi\lambda}\left|\sin\frac{\alpha}{2}\right| + \frac{\tau}{2\pi}\frac{1}{\sqrt{1-m}\,|\sin\frac{\alpha}{2}|}\right)\sqrt{m - \cos^2\frac{\alpha}{2}}, \tag{41}$$

where $\alpha \in (-\pi, -\alpha_1) \cup (\alpha_1, \pi)$, $\alpha_1 = 2\arccos\sqrt{m}$. Now, the normalization condition gives

$$1 = \int_{-\alpha_0}^{\alpha_0} d\beta\rho_{1\,\rm cut}(\beta) = -\frac{2m}{\lambda} + \left(\frac{1}{\sqrt{1-m}} - 1\right)\tau. \tag{42}$$

This uniquely determines m in the interval $0 < m < 1$ for any $\lambda > 0$, $\tau > 0$. Clearly, this density is the same as the density (19), with the argument shifted by π and $\lambda \to -\lambda$ (see Fig. 2). The critical line occurs when $\rho(\pm\pi) = 0$. This gives the condition $4\sqrt{1-m} = \tau\lambda$, which, combined with (42), leads to (40).

[1]The origin of this shift was explained in [4]. It arises from a contribution from the Jacobian of the transformation in going from the real line to the unit circle.

[2]In (19), $\cos\alpha/2$ carries absolute value bars, which can be omitted in the interval $(-\pi, \pi)$. Outside this interval, the density is periodic with period 2π.

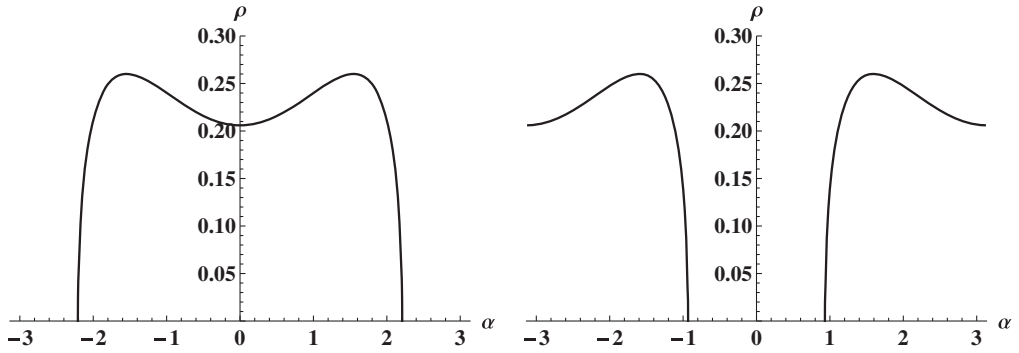

FIG. 2. (a) Eigenvalue density in model A for $\lambda = -3$, $\tau = 1.25$. (b) Eigenvalue density in model B for $\lambda = 3$, $\tau = 1.25$. It differs from the density of (a) by a shift of π.

In the infinite coupling limit, the eigenvalue density assumes the asymptotic form

$$\rho_{1\,\mathrm{cut}}(\alpha)\Big|_{\lambda=\infty} = \frac{\tau}{2\pi}\frac{1}{\sqrt{1-m_\infty}\,|\sin\frac{\alpha}{2}|}\sqrt{m_\infty - \cos^2\frac{\alpha}{2}},$$
$$m_\infty = \frac{1+2\tau}{(1+\tau)^2}. \tag{43}$$

2. Two-cut phase in model B $(0 < \lambda < \lambda_{\mathrm{cr}})$

In the weak-coupling phase, the eigenvalue density has support on two cuts. Applying the map $\lambda \to -\lambda$, $\alpha \to \alpha \pm \pi$ to (25), we get

$$\rho_{2\,\mathrm{cuts}}(\alpha) = \frac{\tau}{4\pi}\sqrt{\sin^2\alpha}\sqrt{a^2 - \cot^2\frac{\alpha}{2}}\sqrt{\cot^2\frac{\alpha}{2} - b^2},$$
$$\lambda < \lambda_{\mathrm{cr}}(\tau), \tag{44}$$

where now

$$\alpha \in (-c_2, -c_1) \cup (c_1, c_2), \qquad c_1 = 2\mathrm{arccot}(a),$$
$$c_2 = 2\mathrm{arccot}(b), \tag{45}$$

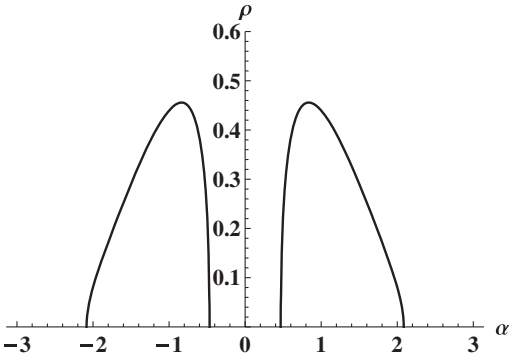

FIG. 3. Eigenvalue density in the two-cut (weak-coupling) phase in model B. Here $\tau = 1$, $\lambda = 0.8$.

$$1 + a^2 = \frac{4(1+\tau+\sqrt{2\tau+1})}{\lambda\tau^2}, \tag{46}$$

$$1 + b^2 = \frac{4(1+\tau-\sqrt{2\tau+1})}{\lambda\tau^2}. \tag{47}$$

One can check that this solves the saddle-point integral equation (39). A plot of the density is shown in Fig. 3.

In the $\lambda \to 0$ limit, the cuts become small with a size scalinglike $\sqrt{\lambda}$ and approach the origin. The eigenvalue density approaches the scaling form

$$\rho_{2\,\mathrm{cuts}}(y)\Big|_{\lambda\to 0} = \frac{1}{\pi|y|}\sqrt{y^2 - c_-}\sqrt{c_+ - y^2}, \qquad y = \frac{\alpha}{\sqrt{\lambda}},$$
$$c_\pm = 1 + \tau \pm \sqrt{1+2\tau}. \tag{48}$$

Summarizing, in the region $\tau > 0$, $\lambda > 0$, model B has two phases: a strong-coupling phase $\lambda > \lambda_{\mathrm{cr}}(\tau)$ described by a one-cut eigenvalue distribution and a weak-coupling phase $\lambda < \lambda_{\mathrm{cr}}(\tau)$ described by a two-cut eigenvalue distribution. In the $\tau = 0$ limit, the eigenvalue distributions

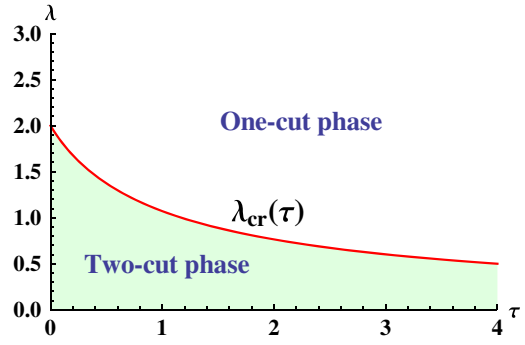

FIG. 4. Phase diagram for model B. The critical line λ_{cr} separates a one-cut phase from a two-cut phase. At $\tau = 0$, it approaches the critical coupling $\lambda = 2$ of the GWW matrix model.

reduce to the ungapped ($\lambda > 2$) and gapped ($\lambda < 2$) eigenvalue distributions of the GWW model. The phase diagram of the theory is shown in Fig. 4.

III. CRITICAL BEHAVIOR OF THE FREE ENERGY AND WILSON LOOPS

Let us now study the analytic properties of the free energy in crossing the critical line. To approach the critical line, τ will be fixed and λ will be increased or decreased. The first derivative of the free energy is directly related to the vacuum expectation value W of the Wilson loop operator corresponding to a single plaquette, $\frac{1}{2N}\mathrm{Tr}(U + U^\dagger)$. One has

$$W = \int_L d\alpha\, \rho(\alpha) \cos\alpha = \frac{\lambda^2}{2N^2}\frac{\partial F}{\partial \lambda} = \langle \cos\alpha \rangle. \quad (49)$$

The second and third derivatives of the free energy can be obtained by further differentiating the VEV of the Wilson loop operator. That is, we will also need

$$\partial_\lambda W, \qquad \partial_\lambda^2 W. \quad (50)$$

The VEV of the Wilson loop was computed in [4] in model A in the region $\lambda > 0$, where the model is in the one-cut phase. This calculation shows that the GWW transition taking place at $\lambda = 2$, $\tau = 0$, becomes a crossover for any $\tau > 0$. As explained above, there is however a phase transition taking place on a critical line at negative λ. For model B, this phase transition occurs in the $\lambda > 0$ region. Below we shall consider this model and compute the Wilson loop and its derivatives in the two phases.

A. Strong-coupling phase

At strong coupling $\lambda > \lambda_{\rm cr}$, the density is given by (41). To compute the integral (49), it is convenient to use the density (19) and then the map $\lambda \to -\lambda$, $\langle \cos\alpha \rangle \to -\langle \cos\alpha \rangle$, the latter induced by the shift in α. An integration by residues then gives

$$W = \frac{1}{\lambda} m(2 - m) - \tau(1 - \sqrt{1 - m}). \quad (51)$$

Here $m = m(\lambda, \tau)$ is obtained as one of the roots of the cubic equation that arises from the normalization condition (42) (we omit the explicit expression). At small τ, the Wilson loop in this phase has the expansion

$$W = \frac{1}{\lambda} - \tau + \frac{\lambda\tau^2}{\lambda + 2} + O(\tau^3), \qquad \lambda > \lambda_{\rm cr}. \quad (52)$$

When $\tau \to 0$, this reproduces the expression for the Wilson loop in the GWW matrix model in the ungapped phase.

One can compute derivatives of W using the chain rule

$$\frac{dW}{d\lambda} = \frac{\partial W}{\partial \lambda} + \frac{\partial m}{\partial \lambda}\frac{\partial W}{\partial m}, \quad (53)$$

etc., where $\frac{\partial m}{\partial \lambda}$ is obtained from the normalization condition (42). In particular, we find the simple formula $\frac{dW}{d\lambda} = -\frac{m^2}{\lambda^2}$. At the critical point,

$$m \to m_{\rm cr} = 1 - \frac{\lambda^2\tau^2}{16}. \quad (54)$$

Using (40) and (54), we obtain the following exact expressions:

$$W(\lambda_{\rm cr}, \tau) = \frac{1}{\tau^2}((1 + 2\tau)^{\frac{3}{2}} - 1 - 3\tau - \tau^2), \quad (55)$$

$$\left.\frac{dW}{d\lambda}\right|_{\lambda_{\rm cr}} = -\frac{1}{4}(1 + 2\tau), \quad (56)$$

$$\left.\frac{d^2W}{d\lambda^2}\right|_{\lambda_{\rm cr}} = \frac{1}{8}(1 + \tau)(1 + 2\tau) + \frac{1}{16}(2 + 4\tau + \tau^2)\sqrt{2\tau + 1}. \quad (57)$$

B. Weak-coupling phase

Let us now consider the two-cut phase described by the eigenvalue density (44). Introducing the variable $t = e^{i\alpha}$ as in Sec. II A 2, the VEV of the Wilson loop can be expressed in terms of the following integral:

$$W = \langle \cos\alpha \rangle = \int_L dt\, \hat{\rho}(t)\frac{1 + t^2}{2t}. \quad (58)$$

In order to compute the integral, we use the shifted density (25) as before, taking into account the map $W \to -W$ and $\lambda \to -\lambda$. We find the following remarkably simple result:

$$W = 1 - \frac{\lambda}{4}(1 + 2\tau), \qquad 0 < \lambda < \lambda_{\rm cr}. \quad (59)$$

For $\tau \to 0$, it reproduces the Wilson loop of the GWW matrix model in the gapped phase.

On the critical line $\lambda_{\rm cr}(\tau)$, W reduces to the same expression (55) of the supercritical phase, so the Wilson loop is continuous across the critical line. Similarly, the first derivative of the Wilson loop matches (56). For the second derivative, we now obtain

$$\left.\frac{d^2W}{d\lambda^2}\right|_{\lambda_{\rm cr}} \equiv 0. \quad (60)$$

Comparing with (57), one finds that the second derivative of the Wilson loop is discontinuous across the transition.

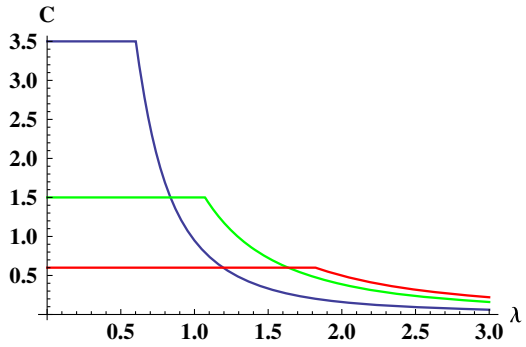

FIG. 5. The specific heat $C/N^2 = -2\partial_\lambda W$ vs λ, for $\tau = 0.1$ (red), $\tau = 1$ (green), and $\tau = 3$ (blue). The discontinuity in the derivative at the critical point shows that the phase transition is third order.

This implies that the third derivative of the free energy is discontinuous. Thus, the system undergoes a third-order phase transition across the critical line represented by $\lambda = \lambda_{\rm cr}(\tau)$. Figure 5 displays the behavior of the first derivative $\partial_\lambda W$, related to the specific heat (viewing the system as a statistical ensemble with temperature $T = \lambda$).

C. Winding Wilson loops

In a similar way, one can compute the vacuum expectation value of winding Wilson loops [5] (see also [22–24]). At large N, they are given by

$$W_k = \frac{1}{2N}\langle \mathrm{Tr}(U^k + U^{\dagger k})\rangle = \int_L d\alpha\, \rho(\alpha)\cos(k\alpha) = \langle \cos(k\alpha)\rangle. \tag{61}$$

We obtain the following results for the two phases:

1. Strong-coupling phase $\lambda > \lambda_{\rm cr}$

$$W_2 = -\frac{2(1-m)^2 m}{\lambda} + \Big((1+m)\sqrt{1-m} - 1\Big)\tau,$$
$$W_3 = \frac{m(1-m)^2(2-5m)}{\lambda} + \Big((2m^2+1)\sqrt{1-m} - 1\Big)\tau, \tag{62}$$

etc. At small τ, they have the expansion

$$W_k = -\tau + \frac{k\lambda}{2+\lambda}\tau^2 + O(\tau^3), \qquad k \geq 2. \tag{63}$$

The W_k's vanish in the limit $\tau \to 0$, in agreement with [5].

2. Weak-coupling phase $\lambda < \lambda_{\rm cr}$

$$W_2 = 1 - \lambda(2\tau+1) + \frac{1}{4}\lambda^2(2\tau^2+3\tau+1),$$
$$W_3 = 1 - \frac{9}{4}\lambda(2\tau+1) + \frac{3}{2}\lambda^2(2\tau^2+3\tau+1) - \frac{1}{16}\lambda^3(8\tau^3+24\tau^2+20\tau+5), \tag{64}$$

etc. One can check that (62) and (64) match on the critical line $\lambda = \lambda_{\rm cr}(\tau)$, whereas the second derivatives of W_k are discontinuous.

IV. THE β FUNCTION

One of the interesting features of the GWW matrix model is that a β function can be constructed for the large N theory through the dependence of the effective 't Hooft coupling on the lattice spacing [5,6]. The properties of the $1/N$ expansion of the β function have been recently discussed in [25]. It turns out that the complete non-perturbative trans-series can be described thanks to the fact that the β function can be expressed in terms of the VEV of $\det U$, which satisfies a differential equation for any value of N. We expect that a similar treatment can be carried out in the deformed GWW model. In this section, we will just focus in the leading large N β function for the models A and B.

In terms of the string tension σ and the lattice spacing a, the Wilson loop has the form

$$W(\lambda,\tau) = e^{-a^2\sigma}. \tag{65}$$

Following [5,6], a running coupling $\lambda(a)$ can be obtained by varying the lattice spacing a keeping σ fixed. This defines an effective coupling $\lambda = \lambda(a;\tau)$. We assume that τ does not renormalize as here it represents the Veneziano parameter N_f/N. The β function for the coupling λ is then obtained by the formula

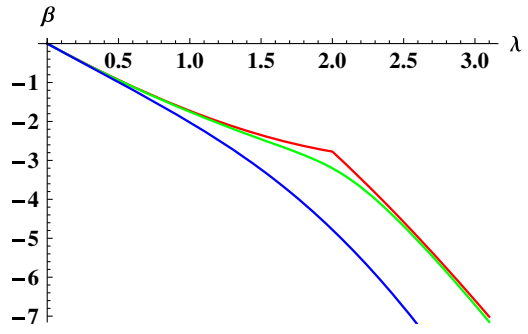

FIG. 6. The β function for model A, for $\tau = 0$ (red), $\tau = 0.03$ (green), $\tau = 0.35$ (blue).

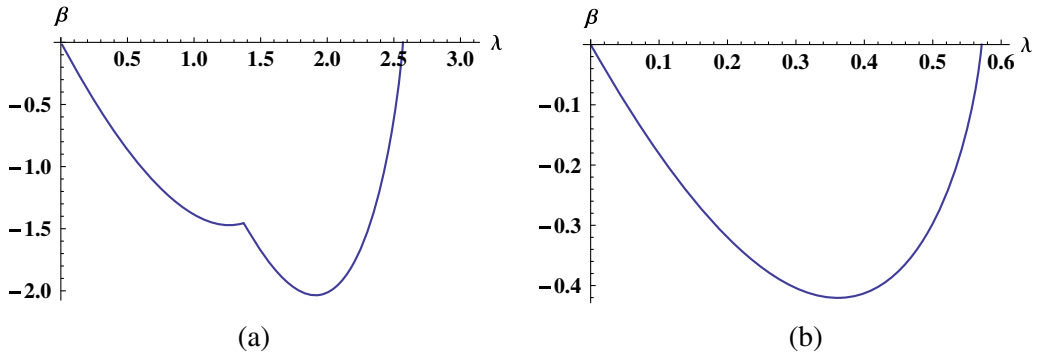

FIG. 7. The β function for model B. (a) $\tau = 0.5$ and (b) $\tau = 3$. In case (b), the fixed point is reached before the critical coupling $\lambda_{\rm cr}$.

$$\beta = -a\frac{\partial\lambda}{\partial a}. \tag{66}$$

This leads to the following expression in terms of the Wilson loop:

$$\beta = -\frac{2W}{\partial_\lambda W}\ln W. \tag{67}$$

A. Model A

In the region $\{\lambda > 0, \tau > 0\}$, model A has only one phase. The Wilson loop has been calculated in [4] and can be obtained from the formulas in Sec. III A by the map $\lambda \to -\lambda$, $W \to -W$. The ensuing β function (67) is plotted in Fig. 6 for different values of τ. One can see that the discontinuous behavior of the $\tau = 0$ GWW matrix theory is smoothed out for finite positive τ.

The β function has the following perturbative (planar) expansion:

$$\beta = -2\lambda + \frac{1}{4}(1-2\tau)\lambda^2 + \frac{1}{48}(1-12\tau)\lambda^3 + O(\lambda^4),$$
$$0 < \lambda \ll 1, \tag{68}$$

where the first term comes from the classical dimension of the coupling.

B. Model B

Model B has two phases in the region $\{\lambda > 0, \tau > 0\}$. In the weak-coupling phase, one can use the results of Sec. III B to derive the following simple formula:

$$\beta = \frac{2}{1+2\tau}(4-\lambda(1+2\tau))\ln\left(1-\frac{1}{4}\lambda(1+2\tau)\right),$$
$$\lambda < \lambda_{\rm cr}(\tau). \tag{69}$$

This has the perturbative expansion

$$\beta = -2\lambda + \frac{1}{4}\lambda^2(2\tau+1) + \frac{1}{48}\lambda^3(2\tau+1)^2 + O(\lambda^4). \tag{70}$$

In the strong-coupling phase, the resulting expression is obtained from (67), where W and $\partial_\lambda W$ can be read from the formulas in Sec. III.1. In either phases, for $\tau = 0$, one reproduces the β function found by Gross and Witten [5].

The β function is shown in Fig. 7 for different values of τ. Comparing with the $\tau = 0$ case, a new feature appears for any $\tau > 0$. The β function now has an IR stable fixed point at finite coupling λ. Coming from $\lambda = 0$, when $\tau < 1 + \sqrt{2}$, the fixed point occurs after the phase transition, that is, in the one-cut (strong-coupling) phase. When $\tau > 1 + \sqrt{2}$, the fixed point occurs before the phase transition has taken place. For small τ, the fixed point occurs at $\lambda^* \approx 1/\tau$, that is, at strong coupling $\lambda^* \gg 1$. This can be seen from the expansion (52). It is important to note that the origin of the fixed point is that $W \to 0$, which is indicative of an infinite string tension, a highly confining regime. This is to be distinguished from a fixed point where $W \to 1$, which would indicate a vanishing string tension and a nonconfining regime, which does not happen in this case (and it is not expected to happen in general in two dimensions).

ACKNOWLEDGMENTS

The author is grateful to M. Tierz and K. Zarembo for valuable comments. We acknowledge financial support from AGAUR (Generalitat de Catalunya) Grant No. 2017-SGR-929, MINECO Grants No. FPA2016-76005-C and No. PID2019–105614 GB-C21.

[1] M. L. Mehta, *Random Matrices* (Academic Press, New York, 1991).

[2] P. J. Forrester, *Log-Gases and Random Matrices*, London Mathematical Society Monographs Series, Vol. 34 (Princeton University Press, Princeton, NJ, 2010).

[3] J. Baik, P. Deift, and T. Suidan, *Combinatorics and Random Matrix Theory*, Graduate Studies in Mathematics, Vol. 172 (American Mathematical Society, Providence, RI, 2016).

[4] J. G. Russo and M. Tierz, Multiple phases in a generalized Gross-Witten-Wadia matrix model, J. High Energy Phys. 09 (2020) 081.

[5] D. Gross and E. Witten, Possible third order phase transition in the large N lattice gauge theory, Phys. Rev. D **21**, 446 (1980).

[6] S. R. Wadia, A study of U(N) lattice gauge theory in 2-dimensions, arXiv:1212.2906.

[7] J. G. Russo, Deformed Cauchy random matrix ensembles and large N phase transitions, J. High Energy Phys. 11 (2020) 014.

[8] L. Santilli and M. Tierz, Exact equivalences and phase discrepancies between random matrix ensembles, J. Stat. Mech. (2020) 083107.

[9] J. A. Minahan, Matrix models with boundary terms and the generalized Painleve II equation, Phys. Lett. B **268**, 29 (1991).

[10] J. A. Minahan, Flows and solitary waves in unitary matrix models with logarithmic potentials, Nucl. Phys. **B378**, 501 (1992).

[11] N. S. Witte and P. J. Forrester, Gap probabilities in the finite and scaled Cauchy random matrix ensembles, Nonlinearity **13**, 1965 (2000).

[12] S. Huang, J. W. Negele, and J. Polonyi, Meson structure in QCD_2, Nucl. Phys. **B307**, 669 (1988).

[13] T. Eguchi and H. Kawai, Reduction of Dynamical Degrees of Freedom in the Large N Gauge Theory, Phys. Rev. Lett. **48**, 1063 (1982).

[14] H. Neuberger, Topological effects in matrix models representing lattice gauge theories at large N, Ann. Henri Poincaré **4**, S147 (2003).

[15] P. Kovtun, M. Unsal, and L. G. Yaffe, Volume independence in large N(c) QCD-like gauge theories, J. High Energy Phys. 06 (2007) 019.

[16] B. Bringoltz, M. Koren, and S. R. Sharpe, Large-N reduction in QCD with two adjoint Dirac fermions, Phys. Rev. D **85**, 094504 (2012).

[17] M. Creutz, *Quarks, Gluons and Lattices* (Cambridge University Press, Cambridge, United Kingdom, 1983).

[18] B. Sundborg, The Hagedorn transition, deconfinement and $N = 4$ SYM theory, Nucl. Phys. **B573**, 349 (2000).

[19] O. Aharony, J. Marsano, S. Minwalla, K. Papadodimas, and M. Van Raamsdonk, The Hagedorn-deconfinement phase transition in weakly coupled large N gauge theories, Adv. Theor. Math. Phys. **8**, 603 (2004).

[20] L. Alvarez-Gaume, P. Basu, M. Marino, and S. R. Wadia, Blackhole/string transition for the small Schwarzschild Blackhole of $AdS_5 \times S_5$ and critical unitary matrix models, Eur. Phys. J. C **48**, 647 (2006).

[21] S. Mizoguchi, On unitary/Hermitian duality in matrix models, Nucl. Phys. **B716**, 462 (2005).

[22] K. Okuyama, Wilson loops in unitary matrix models at finite N, J. High Energy Phys. 07 (2017) 030.

[23] P. Rossi, M. Campostrini, and E. Vicari, The large N expansion of unitary matrix models, Phys. Rep. **302**, 143 (1998).

[24] E. Alfinito and M. Beccaria, Large N expansion of Wilson loops in the Gross-Witten-Wadia matrix model, J. Phys. A **51**, 055401 (2018).

[25] A. Ahmed and G. V. Dunne, Non-perturbative large N transseries for the Gross–Witten–Wadia beta function, Phys. Lett. B **785**, 342 (2018).